Nonlinear Processes in Geophysics (1995) 2: 269 - 279

Nonlinear Processes in Geophysics

Models of explosive volcanism

A. W. Woods[1], S. M. Bower[1] and M. I. Bursik[2]

[1] Institute of Theoretical Geophysics, DAMTP, Silver Street, Cambridge, CB3 9EW, U.K.
[2] Department of Geology, State University of New York, Buffalo, New York, USA

Received 29 September 1994 - Accepted 11 January 1995 - Communicated by D. Sornette

Abstract. We describe a series of models which illustrate the controls upon the evolution of an erupting mixture of ash and gas during an explosive volcanic eruption. For large eruption rates, material typically issues from a crater as a supersonic jet which may entrain and heat sufficient air to become buoyant and form a Plinian eruption column. If a buoyant eruption column is able to form, then this column may ascend to heights of order 10-30 km, depending upon the erupted mass flux. In contrast, for low eruption rates, a shock forms in the crater and the material issues as a slow subsonic flow which generates dense hot ash flows. A new model shows that as such ash flows propagate from the vent, the density of the flow decreases mainly due to sedimentation, until ultimately the residual ash flow becomes buoyant. The distance the flow travels before becoming buoyant increases with the mass flux in the current and the mean size of particles in the current, but decreases with the flow temperature. It also depends upon the mass of air entrained into the collapsing fountain. The mass fraction of solid lifted from such ash flows into the ascending cloud depends mainly upon the mass of air entrained into the collapsing fountain near the volcanic vent. We apply our models to predict run-out distances and deposition patterns produced by erupting volcanoes.

1 Introduction.

Over the past few years it has become clear that the mechanism of emplacement of hot ash and pumice during explosive volcanic eruptions is complex, and depends upon the geometry of the volcanic vent and crater from which the material issues and the mass fraction of water originally in the magma. Observations of the eruptions of Ngauruhoe 1973 (Nairn and Self, 1978); Mt St Helens on May 18 1980 (Lipman and Mullineaux, 1981; Sparks et al., 1986); the April 1990 eruptions of Mt Redoubt (Woods and Kienle, 1994), and the 1991 eruption of Mt Pinatubo suggest that, in many eruptions, the evolution of the erupted material is complex. In some cases the material issues at high speed from the volcano and, as it entrains and heats air, the density of the bulk mixture falls below the ambient density; in this way a large convecting Plinian eruption column may form directly above the vent. In other cases, the material forms a dense fountain above the vent. Large, hot ash flows then propagate laterally over the surrounding terrain. As these ash flows propagate from the vent, they entrain and heat air, and sediment particles, so that the residual mixture may eventually become buoyant. At this stage, such flows lift off the ground and form coignimbrite eruption columns (Woods and Wohletz, 1991). Coignimbrite eruption columns are able to inject large quantities of fine ash high into the atmosphere, in a similar fashion to their Plinian counterparts (figure 1).

In this paper we present a synthesis of some recent work which has been directed at understanding the controls upon whether a Plinian column or a dense ash flow develops, and the controls upon the dynamics of such ash flows. We commence with a description of the eruption of magma from a volcanic vent and its subsequent decompression through a volcanic crater; following Woods and Bower (1994) we identify conditions under which the flow issuing from a crater is sub- and super-sonic. We then discuss how these dense jets issuing from the crater develop as they ascend into the atmosphere, using the eruption column model of Woods (1988). Coupling the eruption conditions prescribed by the model of the volcanic crater with this eruption column model, we present a series of possible scenarios of eruption evolution, distinguishing the different mechanisms of collapse in low and high mass flux eruptions. We then move on to describe the dynamics of dense, hot ash flows. Using a new model, we calculate the mass fraction of erupted solid which may be elutriated from the flow and the typical travel distance of such a flow as a function of the

Correspondence to: A. W. Woods

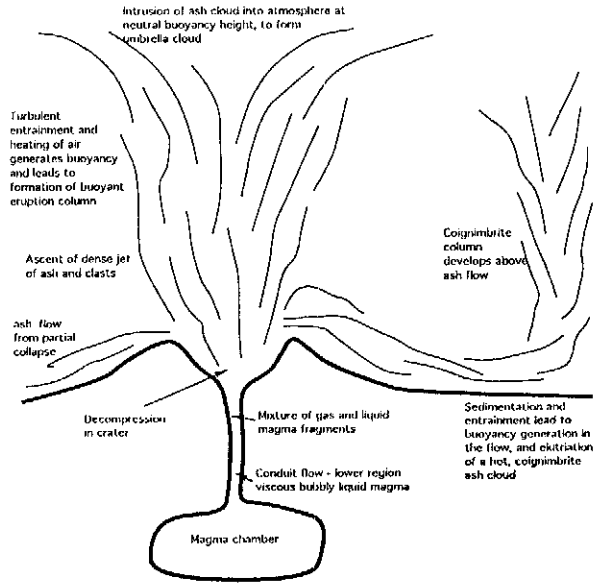

Fig. 1. Schematic of volcanic system

eruption rate, the mass of air entrained into the fountain, and the temperature and the mean grain size of the flow. This provides the source conditions for the coignimbrite eruption columns which may rise from the flow.

2 Magma ascent to the volcanic vent.

At high pressure, in a crustal magma reservoir 3-10 km below the surface, there may be small quantities of water (1-5 wt%) in solution in the magma. During an eruption, this magma rises to the surface and decompresses, due to both gravitational forces and the friction on the walls of the conduit. This pressure loss reduces the solubility of the water in the magma, and vapour bubbles nucleate and grow in the magma. With continued decompression, the magma inflates to become a foamy viscous liquid in which the connected phase is the liquid magma. Once the material has decompressed sufficiently that the volume fraction of gas in this foamy magma exceeds about 70-80%, then a large number of the gas bubbles disrupt (Sparks, 1978). Eventually, a sufficient number of bubbles disrupt that the gas becomes the connected phase. This gas is laden with fragments of vesicular magma, which ultimately become the volcanic ash and pumice. Since the density of the dusty gas mixture is smaller than of the surrounding rock, the pressure loss due to the combination of gravitational and frictional effects is less than the lithostatic pressure gradient of the host rock. Therefore, the mixture typically issues from the vent as an overpressured jet, at pressures 10-100 times atmospheric, and with the speed of sound of the mixture. Models of the flow in the conduit below the crater predict the vent pressure, and hence mass eruption rate, as a function of the vent radius (Wilson et al., 1980; Dobran 1992; Woods and Bower, 1995). Figure 2 shows particular calculations from the model of Woods and Bower (1995). Other than vent radius, the dominant control on the eruption rate is the magma volatile content (figure 2).

The speed of the mixture may be shown to have the approximate value (Woods and Bower, 1994)

$$u_c = (n_o RT)^{1/2} \qquad (1)$$

where n_o is the mass fraction of water (volatiles) mixed with the magma, R is the vapour gas constant, 462 J/kg/K, and T is the eruption temperature, of order 1000K. The vent velocity is nearly independent of the vent pressure. However, the density of the mixture increases with vent pressure, and therefore the erupted mass flux also increases with vent pressure.

3 Crater flow.

In many eruptions, the upper part of the volcano is eroded by this high pressure, dense jet leading to the formation of a crater above the vent (figure 1). The sonic, overpressured jet may therefore partially decompress in this crater before issuing into the atmosphere,

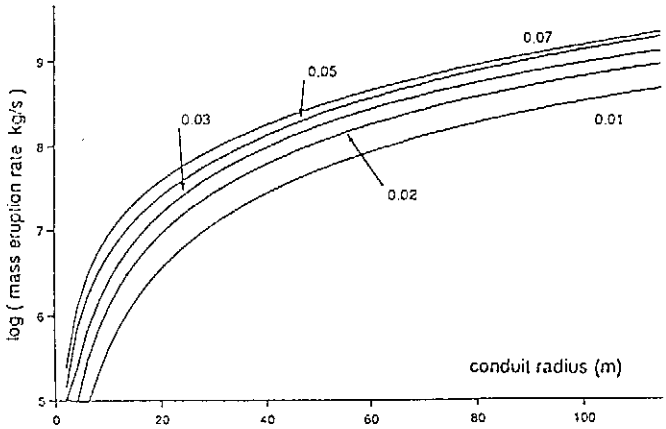

Fig. 2. Relationship between the eruption rate and the conduit radius as a function of the mass fraction of volatiles (water) in the magma.

in an analogous fashion to a jet issuing from an expanding nozzle (Shapiro, 1953). As the material rises in the conduit and crater, the solid/liquid magma typically constitutes of order 95-99% of the total mass. Therefore, even though the gas expands, the mixture does not cool significantly since most of the thermal energy of the mixture lies within the solid (Wilson et al., 1980). It has been shown that the material is therefore approximately isothermal during this decompression (Buresti and Casarosa, 1989).

As the material ascends through the crater of cross-sectional area A, the one-dimensional steady-state conservation of mass and momentum of the mixture may be expressed by the relations

$$u\rho A = Q \quad ; \quad \rho u\frac{du}{dz} + \frac{dp}{dz} = -\rho g \qquad (2,3)$$

where u is the velocity, p the pressure and ρ the density of the mixture, and g is the gravitational acceleration. Here, we assume the crater diverges at a sufficiently

small angle, $< 30°$, that the jet does not separate from the walls of the crater. A simple scaling shows that the frictional drag from the walls of the crater is negligible (Kieffer, 1982). The density is defined in terms of the mass fraction of gas in the mixture, n, and the solid density σ according to the relation

$$\frac{1}{\rho} = \frac{nRT}{p} + \frac{1-n}{\sigma} \qquad (4)$$

Typically, the crater area increases with height above the vent, and so the flow in the crater becomes supersonic directly above the vent. Therefore, the flow at the rim of the crater must either be supersonic or, if the flow in the crater becomes sufficiently underpressured that a shock forms, then the flow at the crater rim should be subsonic and at atmospheric pressure. If a shock forms, so as to recompress the material, and cause a transition from super- to sub-sonic flow, then, across the shock, the mass and momentum fluxes are conserved:

$$[\rho u] = 0 \qquad [\rho u^2 + p] = 0 \qquad (5)$$

The location of the shock is determined by the requirement that the pressure at the crater rim is atmospheric.

Solution of equations (2-5) for a typical crater with walls of inclination 10° and depth 100m shows that three styles of behaviour are possible as a function of the mass flux and hence pressure of the material erupting from the vent (figure 3). For low vent overpressures, the material may become underpressured in the crater, leading to formation of a shock. This recompresses the mixture which then rises at very low sub-sonic speeds (curve iii, figure 3). For larger vent pressures, the material remains supersonic, but issues at a pressure lower than that of the atmosphere (curve ii, figure 3). Finally, for much higher vent pressure, and hence eruption rate, the material remains supersonic and overpressured throughout the crater (curve i, figure 3) (*cf.* Woods and Bower, 1994).

Using this crater flow model, together with the source conditions at the vent (figure 2), we can predict the velocity of the jet issuing from the top of the crater as a function of the crater geometry and the mass eruption rate (figure 4, dotted lines). There is a sharp increase in this velocity at the transition from sub- to super-sonic flow; eruptions with a high mass flux have a large supersonic eruption velocity, while eruptions with a lower mass flux have much lower, subsonic eruption velocities. It is seen that the velocity also increases with magma water content (figure 4).

As the material rises out of the crater, it is free to expand, and will rapidly adjust to atmospheric pressure. This adjustment is complex (Shapiro, 1953). As a very simple model, we assume that the adjustment occurs over a relatively short distance so that the effects of gravity are not important, and we also assume

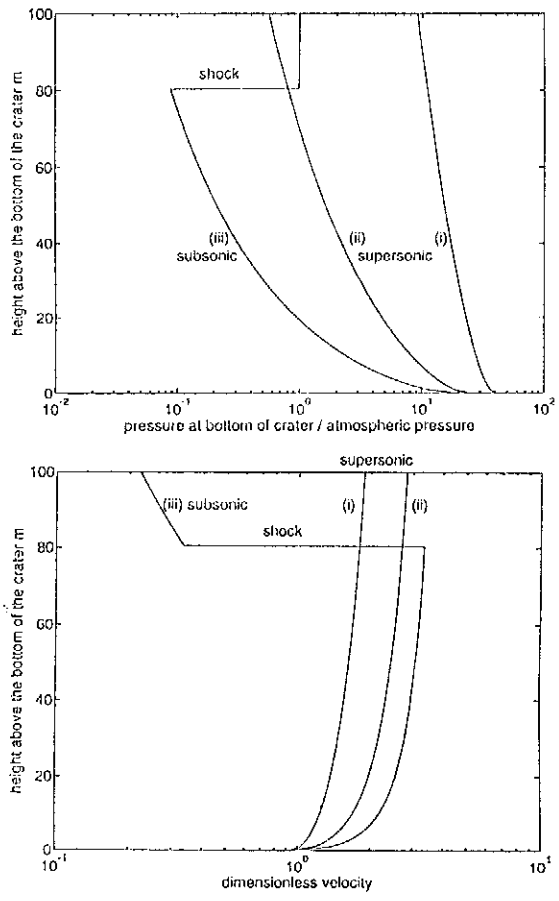

Fig. 3. Variation of (a) pressure and (b) velocity in a crater as a function of the vent pressure. For high vent pressure, curve (i), the flow remains supersonic and overpressured throughout the crater. For intermediate vent pressure, curve (ii), the flow remains supersonic, but becomes underpressured in the crater. For low vent pressure, and hence low eruption rates, curve (iii), the flow becomes so underpressured that a shock forms in the crater, and the flow issues as a pressure adjusted sub-sonic jet.

that there is negligible mixing with the environment during the decompression. In this case, conservation of mass and momentum require that the area and velocity of the fully decompressed jet have the form

$$u = u_c + \frac{A_c(p_c - p_a)}{Q} \qquad \text{and} \qquad A = \frac{A_c \rho_c u_c}{\rho_a u} \qquad (6,7)$$

where ρ_a is the density of the mixture at atmospheric pressure, and subscript c denotes properties evaluated at the crater rim. In figure 4, we also show the velocity of the fully decompressed jet (solid lines) according to equations (6,7) for comparison with the velocity at the crater rim. For the sub-sonic flow the material issues at atmospheric pressure and hence no further adjustment is required.

The subsequent motion of this dense decompressed

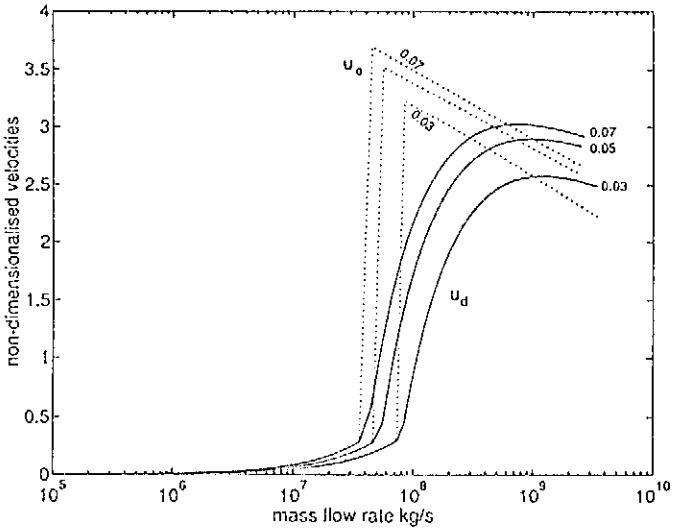

Fig. 4. Velocity of the material at the top of the crater (dashed lines) and after decompression in the atmosphere (solid lines) for three values of the magma volatile mass fraction (0.036, 0.04 and 0.05).

jet then determines the evolution of the erupting material. The main result of this section is that eruptions with low mass flux tend to have low velocity, subsonic jets, while high mass flux eruptions have much higher velocity, supersonic jets.

4 Eruption columns

The erupting mixture of hot ash and gas emerging from the vent feeds a dense upward propagating jet. The upward momentum of this jet decreases owing to the work done against gravity, while the density of the material decreases as it entrains and heats up ambient air. If the material entrains sufficient air before its upward momentum is exhausted then it will generate a buoyant eruption column. Such columns can then inject ash tens of kilometres into the atmosphere. However, if the initial momentum is exhausted before the material has become buoyant then it will generate a dense hot ash flow (Wilson et al., 1980). A fraction of the fine grained material in this dense ash flow may in turn become buoyant and rise from the flow as it continues to entrain and heat air (Sparks et al., 1986). In order to determine critical conditions for collapse of such jets, we use an eruption column model based on the conservation of mass, momentum and enthalpy in the jet. In this section we describe the motion of such jets to develop the basic principles of eruption column behaviour; in the following section, we couple this model with the source conditions described earlier.

The eruption column model assumes that the material is well-mixed at each height, and characterises the properties of the plume with a mean value for that height; the so-called 'top-hat' model. Mass conservation in an eruption column includes a parameterisation of the rate of entrainment of ambient air (Morton et al., 1956; Woods, 1988; Woods 1993) and has the form

$$\frac{d\beta u L^2}{dz} = 2\epsilon L u \alpha \tag{7}$$

where α is the ambient density, L the column radius, u the column velocity and β the column density. The entrainment assumption is equivalent to requiring that air is entrained into the column with velocity ϵu. In the lower part of the column, in which the material is dense relative to the ambient, the entrainment coefficient has the approximate form $\epsilon = 0.09(\beta/\alpha)^{1/2}$ which accounts for the different efficiency of entrainment when there is a large density contrast between the jet and the surrounding fluid (Woods 1988). Once the material becomes buoyant, the entrainment coefficient approximates the value $\epsilon = 0.09$, as in a buoyant plume (Morton et al., 1956). The conservation of momentum has the form

$$\frac{du^2\beta L^2}{dz} = g(\alpha - \beta)L^2 \tag{8}$$

and the steady flow energy equation, which determines the temperature evolution of the column, is given by (Shapiro, 1953; Woods 1988)

$$\frac{du\beta L^2(C_v T + \frac{P}{\rho} + \frac{u^2}{2} + gz)}{dz} = 2\epsilon u L(C_v T_e + \frac{P}{\rho} + \frac{\epsilon^2 u^2}{2} + gz) \tag{9}$$

When these equations are coupled with a model of the standard atmosphere, we can predict the upward speed of the material as a function of the eruption velocity, mass flux, temperature and volatile content (Woods, 1988).

Solutions of this system show that for a given mass flux there is a minimum velocity which will lead to generation of a buoyant column. The critical velocity depends on the eruption rate as well as the mass fraction of water which has exsolved from the magma (figure 5). As the eruption rate increases, more air must be entrained to generate a buoyant column. Therefore, to become buoyant, the material requires a greater initial velocity. Also, as the initial gas content of the magma increases, the critical velocity required to form a buoyant plume for a given mass flux decreases, since the initial density of the material is lower (figure 5).

This simple model of the transition from a buoyant plume to a collapsing fountain has been verified quantitatively using an analogue laboratory system in which jets of methanol-ethylene glycol (MEG) were injected into a laboratory tank of fresh water. MEG exhibits a change in density relative to water as it mixes with the water. Therefore, it is able to simulate the transition in a volcanic column from a dense particle laden jet to a buoyant plume, which occurs if the initial velocity of the jet is sufficient (Woods and Caulfield, 1992).

If a buoyant eruption column develops above the vent, then the column is only able to rise to some maximum height because of the stable stratification in the

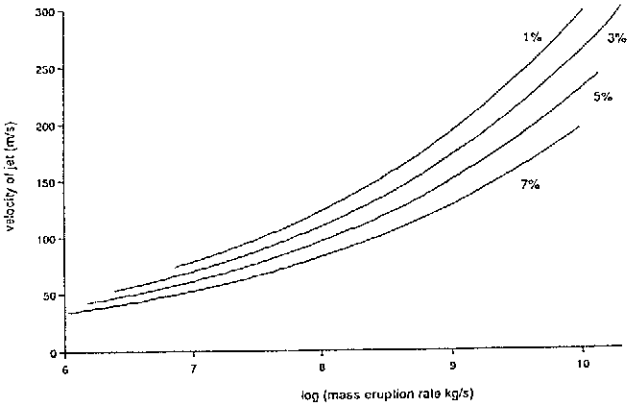

Fig. 5. Critical velocity at which an eruption column can develop as a function of the eruption rate. Curves are given for three values of the magmatic gas content, 0.03, 0.05 and 0.07. The eruption temperature is 1000K.

atmosphere; as the mixture rises, the thermal energy of the ash, which is used to generate the buoyancy by heating entrained air, eventually becomes exhausted and the ash, entrained air and volcanic gases then intrude laterally into the atmosphere. The ascent height of the eruption column primarily depends on the mass eruption rate, the initial temperature of the mixture and the ambient stratification (Wilson et al., 1978; Woods, 1988). In figure 6, we show the predictions of the height of rise of an eruption column as a function of the eruption rate for magma temperatures of 800 and 1200K; further details are given by Woods (1988).

This simple picture of the plume dynamics becomes significantly more complex if the mean grainsize of the ash fragments is large, $\geq$ 1cm, so that they retain much of their heat while ascending in the column. In this case, there is less thermal energy available to heat the entrained air and generate a buoyant column. Many of the larger grain-size fragments fall out of the jet near the vent, leading to the formation of a spatter cone type deposit, and the ensuing eruption column is much smaller or may even collapse (Woods and Bursik, 1991).

In small eruption columns, the model predictions are also sensitive to the moisture loading of the atmosphere. In particular, as the material ascends through the lower atmosphere, it entrains moist air which is then convected higher into the atmosphere, cools, becomes saturated and condenses. The release of latent heat associated with this condensation generates further buoyancy in the eruption column, and may increase the height of rise by a few kilometres in columns smaller than about 10 km (Woods, 1993). The presence of large quantities of condensed water in an eruption column may also lead to the formation of mud-rain.

5 Column Collapse and Eruption Evolution.

In order to determine the eruption style of a hot jet of ash and volcanic gas issuing from a volcano, we must

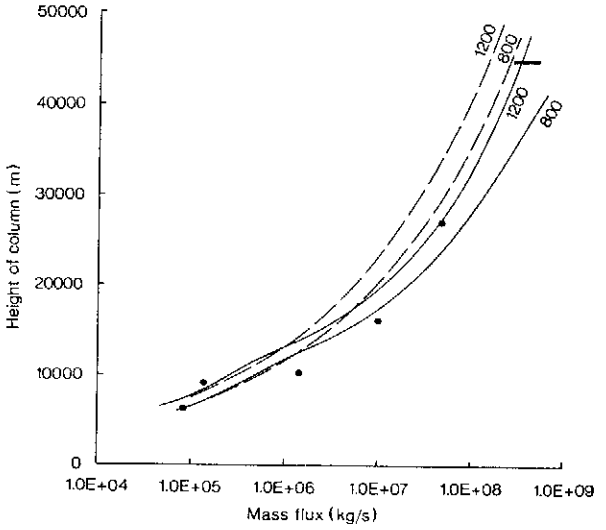

Fig. 6. Height of rise of Plinian eruption columns in a dry environment as a function of the mass eruption rate. Curves are given for two values of the eruption temperature, 800 and 1200K.

couple the source conditions prescribed by the model of decompression in a crater with this eruption column model which predicts whether the material can become buoyant, or collapses to form a dense ash flow. Figure 7 compares the velocity of decompressed volcanic jets issuing from two different sized craters: one with walls of inclination 10 degrees and 100m deep and one with walls of inclination 20 degrees and 500m deep. For the smaller crater, the magma is assumed to have 5wt% volatiles. For the larger crater, the velocity of the jet is shown for magma with both 3 and 5wt% volatiles. The figure also shows the critical velocities for collapse of an erupting jet of magma with 3 and 5 wt% volatiles (cf. figure 5).

By comparing the collapse curve for magma with 3wt% volatiles with the velocity of the decompressed jet of magma with 3wt% volatiles issuing from the larger crater, three different flow regimes may be distinguished. First, at low eruption rates, the velocity of the decompressed jet is slow and subsonic, so that the material is unable to generate an eruption column, and instead it collapses around the volcano, forming a dense ash flow. Second, for intermediate eruption rates, of order 10^7 to 10^{10} kg/s, the material issues from the crater as a much faster, supersonic jet. This is travelling sufficiently fast to generate an eruption column, since the initial velocity exceeds the critical value prescribed by the eruption column model. Finally, for very large eruption rates, in excess of about 10^{10} kg/s, the erupting mass flux is so large that even the supersonic velocity of the erupting material is insufficient to form a buoyant plume before the upward momentum of the material is exhausted. As a result, a dense ash flow is again predicted to form. This lat-

ter style of collapse is comparable to that described by Wilson *et al.* (1980).

The three styles of eruption described above allow us to predict how the behaviour of an erupting jet of ash may evolve during an eruption. First, we mention that many field studies of volcanic deposits suggest that the magma chamber feeding the erupting material is vertically stratified in volatiles. Two such examples include the Lower Bandelier Tuff and the Bishop Tuff (Hildreth, 1979; Anderson et al., 1989; Dunbar and Hervig, 1993, a,b); these deposits indicate

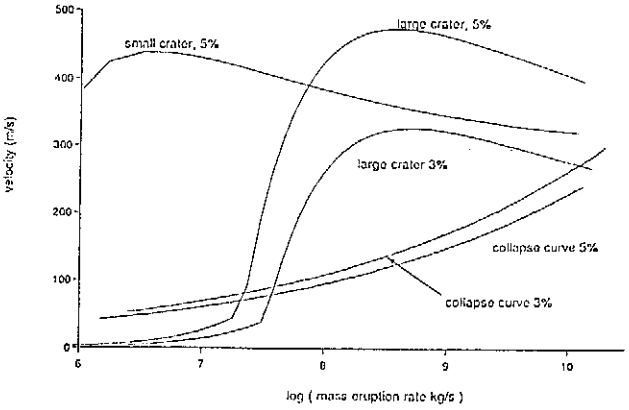

Fig. 7. Comparison of the velocity of a decompressed jet issuing from a crater of depth 100m and angle of inclination 10 degrees (small crater), and a crater of depth 500m and angle of inclination 20 degrees (large crater). For the small crater, the velocity is shown for magma with 5wt% water, while for the large crater the velocity is shown for magma with 3 and 5 wt% water. Also shown on the figure are the critical velocities, predicted by the eruption column model, at which a buoyant eruption column can form (as in figure 5). These curves are shown for magma volatiles contents of 3 and 5wt%.

that the volatile content of the erupting material decreased with time from values of order 5-6 wt% to 2-3 wt%. Secondly, we note that during violent explosive eruptions the crater at the top of the volcanic conduit becomes eroded and enlarged by the high speed ash-laden jet which may be very abrasive (Macedonio *et al.*; 1994).

5.1 Crater erosion.

By comparing the eruption velocities of magma with 5wt% water (volatiles) from small and large craters (figure 7), we deduce that enlargement of a crater can lead to an increase in the eruption rate at which shocks and sub-sonic flow may develop. This increases the minimum eruption rate which can lead to formation of a buoyant eruption column. As a result, an eruption with a relatively small eruption rate may undergo a transition to column collapse purely due to erosion of the crater. The growth of a crater may explain why Plinian eruption columns often collapse in relatively small eruptions ($< 10^8$ kg/s), for which the typical supersonic jet velocities (in the absence of a crater) are always sufficient to form a Plinian column.

5.2 Volatile stratification.

By comparing the eruption velocities of magmas from a large crater with 3 and 5wt% water (figure 7), we deduce that a decrease in the water content, for a given eruption rate, can lead to a decrease in the decompressed jet velocity and an increase in the critical velocity for collapse. As a result the range of eruption rates which lead to formation of a buoyant eruption column becomes smaller. During an eruption with a very large eruption rate, ($> 10^9 - 10^{10}$kg/s) a decrease in the volatile content of the erupting magma may lower the eruption velocity below that required to generate a buoyant column. In this case, the supersonic jet collapses and sheds dense hot ash flows around the volcano. With a much smaller eruption rate ($< 10^6 - 10^7$kg/s), if the volatile content decreases, then a shock may develop within the crater, leading to a transition to sub-sonic flow. Again, this may lead to column collapse and the formation of dense ash flows.

It is important to note that in an eruption of relatively large volatile content, of order 5wt%, column collapse can only develop for very large eruption rates $> 5 \times 10^{10}$ kg/s. Such an eruption rate would be exceptionally large. We deduce that in most eruptions column collapse will be a consequence of either crater erosion (for low mass fluxes) or a decrease in the magma volatile content, with the latter being the most important effect in very large eruptions.

6 Ash flows

If the material collapses to form a dense ash flow, then as this flow propagates it entrains and heats air, and sediments the larger clasts. As a result, a fraction of this solid may become buoyant and rise from the flow, forming a coignimbrite eruption column (figure 1; Woods and Wohletz, 1991). Three notable and recent examples of coignimbrite eruption clouds include the eruption cloud which developed from the lateral blast during the May 18 1980 eruption of Mt St Helens (Sparks et al., 1986), and the ash clouds which developed above the pyroclastic flows during April 1990 at Mt Redoubt, Alaska (Woods and Kienle, 1994) and some stages of the 1991 eruption of Mt Pinatubo. Another example of an eruption in which a large coignimbrite column formed was the great eruption of Tambora (1815) (Sigurdsson and Carey, 1989).

However, in spite of their importance, to date no complete quantitative model has predicted the run-out distance or the mass of solid which may be lifted from such flows. Woods and Bursik (1994) have carried out a series of laboratory experiments, using particle laden currents of fresh water in a tank of saline water, and also using currents of mixtures of methanol and ethlyene glycol (MEG) in a tank of fresh water. The particle experiments examined the role of the sedimentation of clasts upon the dynamics and generation of buoy-

ancy in the flow, and the MEG experiments examined the role of the entrainment and heating of air upon the the flow. Woods and Bursik (1994) showed that the topography of the terrain exerts a strong control upon the relative importance of these two processes. On shallow slopes, the rate of sedimentation from ash flows should dominate, leading to the deposition of much of the material before the flow can become buoyant. However, on very steep slopes, the turbulent entrainment and heating of air may be important, leading to a much larger mass of material becoming buoyant.

Using insight gained from analogue laboratory experiments, we now present a simple model of the motion of a continuous ash flow on a gently sloping terrain, as would develop from a collapsing fountain during a maintained eruption. Our model is based upon the conservation of mass, momentum and energy. We include a parameterisation of the rate of entrainment based on laboratory experiments involving dense currents propagating along sloping boundaries (Turner 1979). We also model the effect of bottom friction on the base of the current using a parameterisation of turbulent drag (Schlicting 1969). Finally, we model the sedimentation of particles following the classical work of Hazen (1904), which has recently been confirmed for laboratory currents of particle laden water propagating along slopes by Woods and Bursik (1994). We restrict attention to currents travelling downslope, with negligible cross-slope spreading, as occurs in a narrow valley or canyon. However the present modelling approach may be extended to more complex and steeply sloping terrains, and to discrete ash flows which result from a short lived explosions such as occured in the eruptions of Mt Redoubt, April, 1990 (Woods and Kienle, 1994).

We assume that the current is in steady state and remains coherent and well-mixed. We denote the mass flux of particles per unit width in the current at position x downstream of the volcano as $Q_s(x) = (1-n)uh\beta$, and the mass flux of air and volcanic volatiles per unit width as $Q_a(x) = nhu\beta$, where n is the gas mass fraction, u is the mean velocity, h the current thickness, and β is the current density. The density is given by eqn (4), using the mass averaged value for the gas constant R of the volcanic gas and entrained air (Woods 1988). The total mass flux per unit width is $Q(x) = Q_s(x) + Q_a(x)$. We assume for simplicity that the rate of sedimentation is given in terms of the mean settling speed of the particles in the current,

$$v_s = \left(\frac{\sigma d g}{\alpha C_D}\right)^{1/2} \tag{10}$$

where d is the characteristic size, $C_D \approx 1$ is a drag coefficient, and $\sigma = 500\text{kg/m}^3$ is the density of pumice clasts, and has the form (Hazen, 1904)

$$\frac{dQ_s}{dx} = -\frac{v_s \cos\theta Q_s}{hu} \tag{11}$$

The term $\cos\theta$ denotes the component of the settling velocity perpendicular to the slope. Equation (11) may be simply extended to account for a grain-size distribution in the flow. The rate of entrainment of air is given by

$$\frac{dQ_a}{dx} = \epsilon\alpha u \tag{12}$$

where α is the ambient density, and the entrainment coefficient $\epsilon(\theta) = 0.09\theta$ on a slope of angle θ (Turner 1979).

The equation for the conservation of momentum has the form

$$\frac{du^2h\beta}{dx} = -g\sin\theta(\alpha-\beta)h - f\beta u^2 \tag{13}$$

where the drag coefficient depends upon the roughness of the bottom boundary, but is of typical magnitude 0.01 (Schlicting 1969). Finally, the steady flow energy equation describes the thermal evolution of the ash flow as it propagates along the ground, entraining cold ambient air, and sedimenting hot particles,

$$\frac{dC_pTuh\beta}{dz} \approx \epsilon\alpha u C_p T_o - v_s\beta(1-n)C_sT \tag{14}$$

Here C_p is the mass averaged specific heat at constant pressure of the flow (Woods 1988), C_s is the specific heat of the solid fragments, T is the temperature of the flow, and T_e is the temperature of the ambient air, set to be 300K in the present model. We neglect the change in potential and kinetic energy in the steady flow equation since in an ash flow they are small compared to the specific enthalpy C_pT.

The motion of such ash flows depends on the initial conditions in the current: the mean grain size, the initial velocity, gas mass fraction and temperature. As cold air is entrained and mixed into the fountain the temperature decreases. Thus the initial gas mass fraction and temperature depend on the amount of entrainment in the collapsing fountain. This has a complex dependence on the initial conditions in the jet issuing from the crater. In particular, as the difference between the actual velocity of the jet and the critical velocity required to form a buoyant column increases, the height of the collapsing fountain decreases, and the initial gas content of the ash flow becomes smaller. We calculate the initial temperature of the mixture feeding the ash flow, T, by conservation of heat, between the erupted material of temperature T_o and the entrained air of temperature T_a, according to

$$T = ((1-\lambda)C_pT_o + \lambda C_aT_a)/((1-\lambda)C_p + \lambda C_a) \tag{15}$$

where λ is the mass fraction of the ash flow composed of air entrained in the flow, and C_p is the bulk specific heat of the erupted magma-volatile mixture.

In the following discussion, we present a series of calculations which illustrate how the dynamics of the

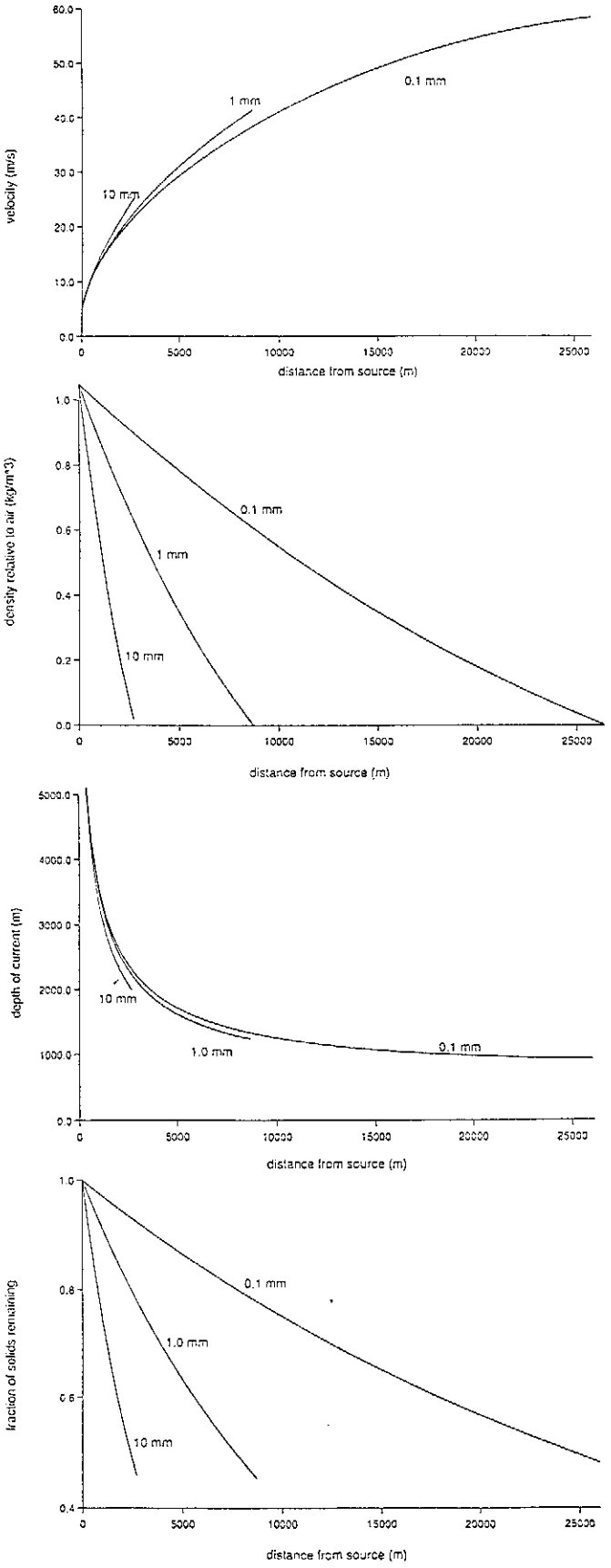

Fig. 8. Predictions of a simple model of an ash flow propagating down the flanks of a volcano. Curves showing the variation of (i) velocity; (ii) density; (iii) fraction of original solid remaining in the flow; and (iv) thickness of the flow for mean grain sizes of 0.1, 1.0 and 10.0 mm. The eruption temperature T_o (eqn 15) is 1000K, the initial air content is assumed to be 10wt%, and the initial velocity is 5m/s. The angle of slope is 1^o.

current depend on the mass of air, λ, the initial eruption temperature, T_o, and the mean grain size of the particles. Figure 8 shows how the current density, velocity, thickness and fraction of solid remaining in the flow change with distance downstream of the volcano. Curves are given for 3 different mean grain sizes in the flow, 0.1mm, 1mm and 10mm, for a typical mass flux of 10^5 kg/s/m issuing from a linear fissure. We assume that the air entrained in the collapsing fountain constitutes 10 wt% of the material feeding the flow ($\lambda = 0.1$). The gas content of the magma issuing from the crater is 5wt%, and the temperature of the mixture before mixing with air in the fountain is $T_o = 1000K$. Finally, the terrain has angle of slope of 1^o. As the grain size increases, the cloud becomes buoyant much closer to the vent because the coarser grained, solid material is deposited nearer to the volcano. Owing to the alongslope acceleration due to gravity, the speed of the flow increases with distance from the volcano and for the most fine-grained current, it attains relatively large values of 50-60m/s when it has travelled 10-15 km from the volcano. The thickness of the current progressively decreases as the current accelerates, since the amount of entrainment is relatively small compared with the mass of the current. Further calculations show that the temperature of the current only decreases by a few tens of degrees on becoming buoyant, since only a relatively small mass of cold air is entrained. Thus, for such shallow slopes, the dominant process controlling the generation of buoyancy is the sedimentation of the particles.

In figure 9 we show how the mass of solid material remaining in the flow and also the run-out distance vary with the mass flux in the current. Curves are given for four values of the mass fractions of air entrained in the fountain, 0, 10, 20 and 30 wt% ($\lambda = 0, 0.1, 0.2, 0.3$), with the initial temperature of the erupting material $T_o = 1000$K. We also show the case of a current with an initial air mass fraction of 10wt% and initial temperature of 800K. The main effect is that the fraction of solid which becomes buoyant increases significantly with the mass of air entrained in the fountain. However, it is also seen that as the initial gas content increases above 10wt% the run-out distance decreases. For the shallow slopes examined here, the entrainment of air into the current itself is relatively small and therefore the air entrained in the collapsing fountain plays a key role in the generation of buoyancy in the flow. Finally, the figure also shows that if the initial temperature of the flow is lower (the curve marked

800K) then the current has to sediment more material and therefore propagates further before becoming buoyant.

In figure 10 we show that, as the mean particle size in the current increases, the distance travelled by the current decreases very significantly owing to the faster rate of sedimentation. However, the fraction of the solid mass which lifts off in the buoyant cloud is relatively insensitive to the mean particle size, since once a sufficient mass of the solid has sedimented, the remaining mixture becomes buoyant.

In summary, figures 9 and 10 show that the run out distance is largely controlled by the mean grain size of the ash flow, while the mass fraction lifted from the flow is most sensitive to the mass of air entrained in the collapsing fountain. The model emphasizes the importance of the sedimentation of particles in controlling the density and hence dynamic evolution of the flow on shallow slopes, and also the importance of the entrainment of air into the collapsing fountain. Although the model is possibly too simplified for a detailed quantitative comparison with field observations, the typical run-out distances and lifted solid fractions predicted by our model are comparable to those obtained from field observations at Mt St Helens, at which the flow travelled 10-20 km at speeds of 50-100m/s and with a thickness of a few hundred metres. Field studies of coignimbrite ash deposits and the associated flow deposits suggest that there is some scatter in the mass fraction of the erupted material elutriated from the flow, although in many cases it lies in the range 20-40% (Sparks and Walker, 1977). Our model predicts that there is a very wide range of solid mass fractions which may be lifted into the buoyant coignimbrite cloud, depending mainly on the mass of air entrained into the fountain and the temperature of the eruption. As the mass of air entrained in the collapsing fountain decreases to values in the range 0-10wt%, the mass fraction of solid which can be lifted in the coignimbrite cloud decreases to values of order 10-40% comparable to the data. Such fountains will develop in eruptions with velocities far below the critical value for collapse; only those fountains which just fail to become buoyant are able to entrain more air, and therefore generate coignimbrite clouds which carry much larger fractions of the erupted solid high into the atmosphere. We note that on larger slopes, and in more discrete ash clouds, such as developed during the eruption of Mt Redoubt, the rate of entrainment of air becomes more important, and the current may be somewhat cooler than for the continuous shallow slope currents described here.

Woods and Wohletz (1991) have shown that the loss of thermal energy associated with the sedimentation decreases the height of rise of the ensuing coignimbrite eruption columns, in comparison with an equivalent Plinian eruption column forming from an eruption of the same mass flux, but different source conditions. Since the height of rise of eruption columns is primarily a function of the mass flux and temperature of the material feeding the flow, we may use figure 6 to deduce the height of rise of a coignimbrite column in terms of the flux and temperature of the material lifted from the flow (Woods and Wohletz, 1991). We deduce that, for a sufficiently large mass flux, even these large coignimbrite eruption columns can penetrate the stratosphere.

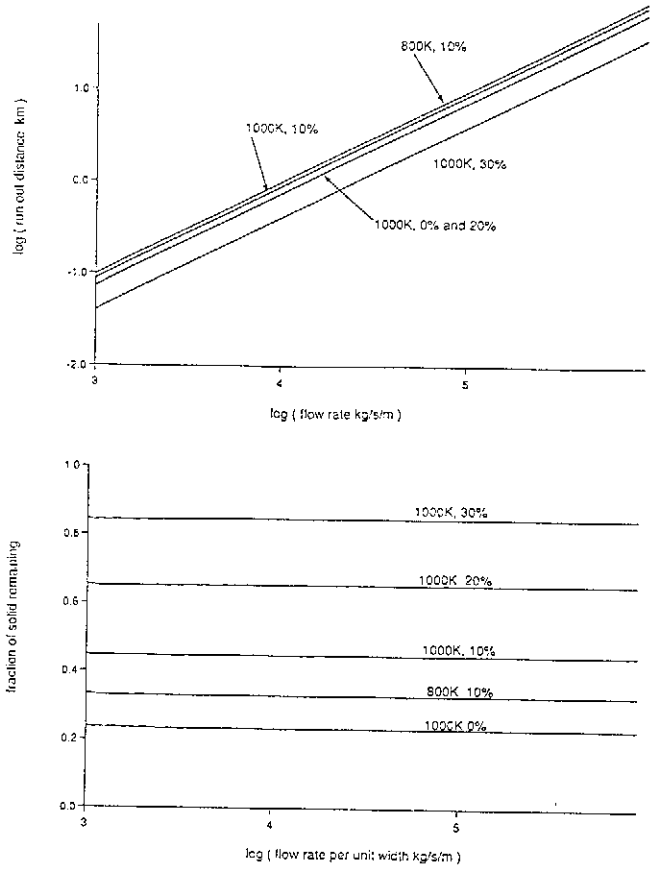

Fig. 9. Predictions of (i) the run-out length and (ii) the mass fraction of solid remaining in the flow as a function of the initial mass flux per unit width of the flow. Curves are shown for a mean grain size of 1mm, an initial velocity of 5 m/s, an eruption velocity of 1000K and an initial air mass fraction of 0, 10, 20 and 30 wt%, corresponding to varying amounts of entrainment in the collapsing fountain. The slope angle is 1° to the horizontal. The final line corresponds to an ash flow with 10wt% gas and an initial temperature of 800K.

7 Summary

In the review part of this paper we have described how molten magma may be injected high into the atmosphere through a series of complex fluid dynamical processes. We have described how material rises through a volcanic crater to the surface and decompresses, either issuing from the crater top at high super-

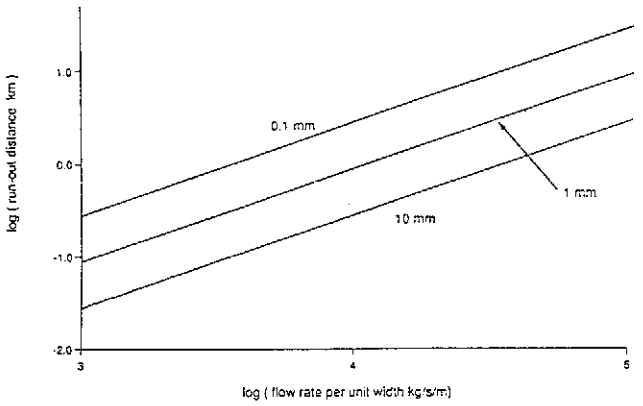

Fig.10. Predictions of the run out length as a function of the mean grain size in the flow and the mass flux per unit width of the flow. Mean grain sizes of 0.1, 1.0 and 10.0 mm are shown, with an initial current velocity of 5m/s, an initial air mass fraction of 10wt%, an eruption temperature of 1000K and an angle of slope of 1°.

sonic speeds or much slower sub-sonic speeds. We have used these source conditions, in conjunction with an eruption column model, to describe conditions under which the jet of erupting material may become buoyant through entrainment and heating of the air, and under which the material remains dense and forms a collapsing fountain above the vent, which then sheds ash flows. For sufficiently low eruption rates, the erosion of a crater or the reduction of the water content of the magma can lead to the formation of a shock in the crater and slow sub-sonic flow. In turn, this produces a collapsing fountain. For high eruption rates, ($> 10^9 - 10^{10}$ kg/s), a reduction of the magmatic water content may also lead to column collapse, since for such high eruption rates the supersonic flow ceases to be sufficiently large to produce a buoyant column.

We have developed a new model of the ash flows which develop from collapsing fountains, including the effects of sedimentation of particles, entrainment of air, and bottom drag. Our model shows that, as an ash flow propagates from the vent, it sediments particles and the density of the material eventually decreases below that of the environment. As a result a large ash cloud may rise from the flow. Our model calculations show that the run-out distance of an ash flow depends mainly on the mean grain size of particles in the flow, while the mass fraction of solids elutriated from the flow depends mainly upon the mass of air entrained in the collapsing fountain. In an eruption whose velocity is much smaller than that required to generate a buoyant plume, the mass of air entrained in the fountain is relatively small, and our model predicts that in this case about 10-40wt% of the erupted solid may rise in the coignimbrite cloud, in accord with field estimates.

Developments of these models will include examining the effects of (i) a distribution of grain sizes, and therefore a range of sedimentation rates; (ii) the effects of thermal disequilibrium in ash flows; and (iii) the effects of more complex topography, flow geometry and source conditions on the dynamics of the flows.

References.

Anderson, A.T., Newman, S., WIlliams, S.N., Druitt, T., Skirius, C., and Stolper, E., 1989, H_2O, CO_2, Cl and gas in Plinian and ash flow Bishop ryholite, Geology, 17, 221-225

Bursik, M.I. and Woods, A.W., 1991, Buoyant, Superbuoyant and collapsing eruption columns, J. Volc. Geotherm. Res., 45, 347-350

Buresti, G and Casarosa, C., 1989 One dimensional adiabatic flow of equilibrium gas-particle mixtures in long vertical ducts with friction, J Fluid Mech., 203, 251-272

Carey, S. and Sigurdsson, H., 1987, Temporal variations in column height and magma discharge rate during the AD 79 eruption of Vesuvius, Geol. Soc. Am. Bull., 99, 303-314

Dobran, F. 1992, Non-equilibrium flow volcanic conduits and application to the eruptions of Mt St Helens on May 18 1980 and Vesuvius in AD79, J Volc Geotherm Res., 49, 285-311

Dunbar, N and Hervig, 1992 a Volatile and trce element composition of melt inclusions from the lower bandelier tuff: implications for magma chamber processes and eruptive style, J Geophys Res., 15151-15170

Dunbar N and Hervig 1992 b Volatile and trace element composition of melt inclusions from the lower bandelier tuff, implications for eruptive stle and magma chamber processes, J Geophys Res, 15171-15185

Hazen, A., 1904, On sedimentation, Trans Am Soc Civ Eng, 53, 45-88

Hildreth, W., 1979, The Bishop Tuff: Evidence for the origin of compositional zoning in silicic magma chambers, Geological Soc. Am. Special Paper, 180, 43-75

Jaupart, C. and Tait, S., 1990, Dynamics of eruptive phenomena, chap 8, in Reviews in Mineralogy. Ed. J. Micholls and J. Russel, Rev. Min., 24, 213-238.

Kieffer, S., 1982, Fluid dynamics and thermodynamics of Ionian volcanism, Chap 18, in Satellites of Jupiter, Ed. Morrison, D., University of Arizona Press, Tucson, 1982

Koyaguchi, T. and Woods, A.W., 1994, On the dynamics of explosive eruptions of magma and water, sub-judice

Lipman, P.W. and Mullineaux, D.R, 1981, The 1980 eruptions of Mt St Helens, U.S. Geol. Surv. Prof. Pap. 1250, 1981

Macedonio, G, Dobran F. and Neri A, 1994, Erosion processes in volcanic conduits and an application to the AD79 eruption of Vesuvius, Earth Planet Sci Lett, 121, 137-152

Morton, B., Taylor, G.I., Turner, J.S., 1956, Gravitational turbulent convection from maintained and instantaneous sources, Proc. R. Soc., Lond., A, 234, 1-23

Nairn, I and Self, S 1978, Explosive eruptions and pyroclastic avalanches from Nguaruhoe in February 1975, J Volc Geotherm Res., 3, 39-60

Schlicting, A., Boundary layer theory, McGraw Hill, 1969

Settle, M., 1978, Volcanic eruption clouds and the them ral power output of explosive eruptions, J Volc. Geotherm Res., 3, 309-324

Shapiro, A., 1953, The dynamics and thermodynamics of compressible fluid flow, Wiley, New York, 647.

Sigurdsson, H. and Carey, S., 1989, The 1815 eruption of Tambora volcano, Bull Volcanol., 51: 243-270

Sparks, R.S.J., 1978, The dynamics of bubble formation and growth in magmas, J. Volc. Geotherm. Res., 3, 1-37

Sparks R.S.J. and Walker G.P.L. 1977 On the significance of vitric enriched air-fall associated with crystal-enriched ignimbrites, J Volc Geotherm. Res., 2, 329-341

Sparks, R.S.J., Moore, J.G., Rice, C., 1986, The initial giant umbrella cloud of the May 18 1980 explosive eruption of Mt St Helens, J. Volc. Geotherm. Res.,28, 257-274

Turner, J.S., Buoyancy effects in fluids, Cambridge Univ. Press., 1979.

Woods, A.W. and Caulfield, C.P., 1992, A laboratory study of explosive volcanic eruptions, J. Geophys. Res., 97, 6699-6712

Woods, A.W. and Bursik, M.I., 1991, Particle fallout, thermal diqequilibrium and volcanic plumes, Bull. Volcanol., 53, 559-570

Woods, A.W. and Bursik, M.I., 1994, A laboratory study of ash flows, J. Goephys. Res., 99, 4375-4394

Woods, A.W., 1993, Moist convection and the injection of volcanic ash into the stratosphere, J. Goephys. Res., 98, 17,627-17636

Woods, A.W. and Wohletz, K., 1991, The dimensions and dynamics of coignimbrite eruption columns, Nature, 350, 225-227

Woods, A.W. and Bower, S., 1994, On the decompression of volcanic jets, sub-judice

Woods, A.W., and Kienle, J., 1994, The thermodynamics and fluid dynamics of volcanic clouds: Observations of Mt Redoubt, April 21, 1990, in press, J. Volc. Geotherm. Res.

Wilson, L., Sparks, R.S.J., Huang, T. and Watkins, N., 1978, The control of eruption heights by eruption energetics and dynamics, J. Geophys, Res., 83, 1829-1836

Wilson, L., Sparks, R.S.J., and Walker, G.P.L., 1980, Explosive volcanic eruptions: The control of magma properties and conduit geometry upon eruption column behaviour, Geophys. J. Roy. Astr. Soc., 63, 117-148

Woods, A.W., 1988, The fluid dynamics and thermodynamics of eruption columns, Bull. Volcanol., 50, 69-91